JOURNAL OF MATERIALS SCIENCE: MATERIALS IN MEDICINE 12 (2001) 283–292

Evaluation of mechanical and corrosion biocompatibility of TiTa alloys

E. A. TRILLO, C. ORTIZ, P. DICKERSON, R. VILLA, S. W. STAFFORD, L. E. MURR
Department of Metallurgical and Materials Engineering, The University of Texas at El Paso, El Paso, Texas 79968, USA

As-received and heat-treated Ti40Ta and Ti50Ta alloys were evaluated to determine their corrosion as well as mechanical performances and compared to Ti6A14V, a common material utilized for orthopedic (surgical) implants. Anodic potentiodynamic tests performed in Plasmalyte™ showed that all samples, except for the Ti50Ta specimen aged at 400 °C for 3 h gave a curve similar to that of Ti6A14V. Optical and TEM microscopy was performed to determine as-received and heat-treated microstructures. As-received materials showed an α precipitate in an $\alpha + \beta$ and martensite matrix. Samples that were aged at 400 °C increased in the density and the length of the α precipitate. Vickers hardness measurements were performed to get an approximation of the tensile strengths. Aged Ti40Ta and Ti50Ta specimens produced the highest tensile values when compared to the Ti6A14V material, representing a 31% and 56% increase for the 3 h samples and an 18% and 58% increase for the 10 h samples. Of all the materials studied the Ti50Ta specimen aged for 10 h exhibited the best biocompatibility showing excellent corrosion resistance combined with the highest tensile strength (1089 MPa and 58% harder/stronger than Ti6A14V).

1. Introduction

Metallic implant materials such as commercially pure (CP) Ti and Ti6A14V have experienced a trend of growing interest especially as orthopedic and surgical reconstructive implants. Their high corrosion resistance and strength-to-weight ratio properties make them ideal materials for bioimplantation. In addition, these materials exhibit relatively high fatigue strengths and are nonthrombogenic.

Of recent concern, however, is the presence of Ti ions that have appeared in several clinical studies involving Ti6A14V and CP Ti [1–8]. In large amounts Ti may hinder the recovery process by increasing the amount of local inflammation. With current trends leaning toward longer implantation times and larger surface areas the issue of Ti toxicity becomes a real concern.

It is the aim of this paper to determine the biocompatibility of two Ti-Ta alloys (Ti40Ta and Ti50Ta) as potential replacements for the current Ti alloys. Tantalum is currently used in surgeries involving vascular axes and secretory canals [9, 10] and is also a material that exhibits high corrosion resistance. Few researchers have performed biocompatibility studies on Ti-Ta alloys and have mainly centered their efforts on Ti5Ta [11]. In this study, anodic polarization curves were performed on the two alloys to determine passive behavior under several different heat-treatment conditions. Optical as well as transmission electron microscopy (TEM) have been performed to characterize the resulting heat-treated microstructures. Vickers microhardness tests were performed to monitor aged microstructural variations and to obtain an estimate of the tensile strengths of all the samples.

2. Experimental procedures

The Ti40Ta and Ti50Ta materials were received in billet form and had compositions like those listed in Table I. The major alloying elements are Ti and Ta with some trace impurities of Fe, Si, Al and C. Samples of approximately 0.6 cm diameter disk areas were sectioned. Ti6A14V samples were also sectioned from rod material and was used in these experiments as a biomaterial control.

Four different heat-treatments were carried out on all three materials. Set one was heat-treated to 1000 °C for 1 h and then water quenched. Set two was carried out at the same temperature and time but furnace cooled. Set three was aged at 400 °C for 3 h and then water quenched. Set four was aged at 400 °C for 10 h and then water quenched. All heat-treatments were carried out in an Ar atmosphere.

Samples were mechanically polished using SiC paper and then fine polished with 1.0 micron and 0.3 micron alumina slurries, and then colloidal silica. Samples were then washed in a mild soap solution and rinsed thoroughly with distilled water and ethanol.

Potentiodynamic tests were then performed on all samples using Plasmalyte™, a simulated biological solution at 0.17 m V/s *vs* SCE. Scans were run only on the anodic side of the potentiodynamic curve to compare the passive behaviors of the materials. Samples were then

TABLE I Alloy composition (%)

	Ta	Fe	Si	Al	C	Ti
Ti40Ta	37.8	0.18	0.1	0.05	0.01	Balance
Ti50Ta	45.6	0.4	0.18	0.05	0.01	Balance

chemically polished in preparation for optical microscopy. The chemical polish solution consisted of 25 ml lactic acid, 15 ml HNO_3 and 5 ml HF. To further enhance grain structure an etching solution of 20 ml HNO_3, 20 ml HF and 60 ml H_2SO_4 was utilized. In some instances, a stronger etching solution of 80% HF in H_2O was utilized.

Thin sections were then obtained for TEM. Three mm discs were punched from approximately 200 μm thick foils of all the materials. The jet polishing solution consisted of 150 ml HCl, 50 ml HF and 1400 ml methanol at 10 °C. A Hitachi H-8000 Scanning Transmission Electron Microscope operating at 200 kV was used in order to observe internal microstructure.

An estimate of the tensile strengths of the Ti-Ta alloys was obtained from Vickers microhardness data. These values were also converted to Brinell hardness and then multiplied by a factor of 350 (used for non-ferrous alloys) to obtain approximate tensile strengths in psi.

3. Results

The anodic polarization curves for the as-received as well as 1000 °C heat-treated samples are recorded in Figs 1 and 2. All samples show that a stable passive layer has formed on the material surface at low current densities. The as-received Ti40Ta (Fig. 1a) and Ti50Ta (Fig. 1b) materials exhibit the same kind of polarization slope as that of Ti6A14V (Fig. 1c) which was included as a biomaterial standard reference. The samples that have been heat-treated at 1000 °C and quenched (Fig. 2a and b) and furnace cooled (Fig. 2c and d) show a much steeper passive slope yet exhibit a passive current density of approximately $1 \times 10^{-1} \mu A/cm^2$ similar to the as-received Ti6A14V sample.

The aged samples (400 °C) display a variation in polarization curves. Although the Ti40Ta sample treated for 3 h (Fig. 3a) has a stable passive layer it occurs at a higher current density than the as-received and 1000 °C

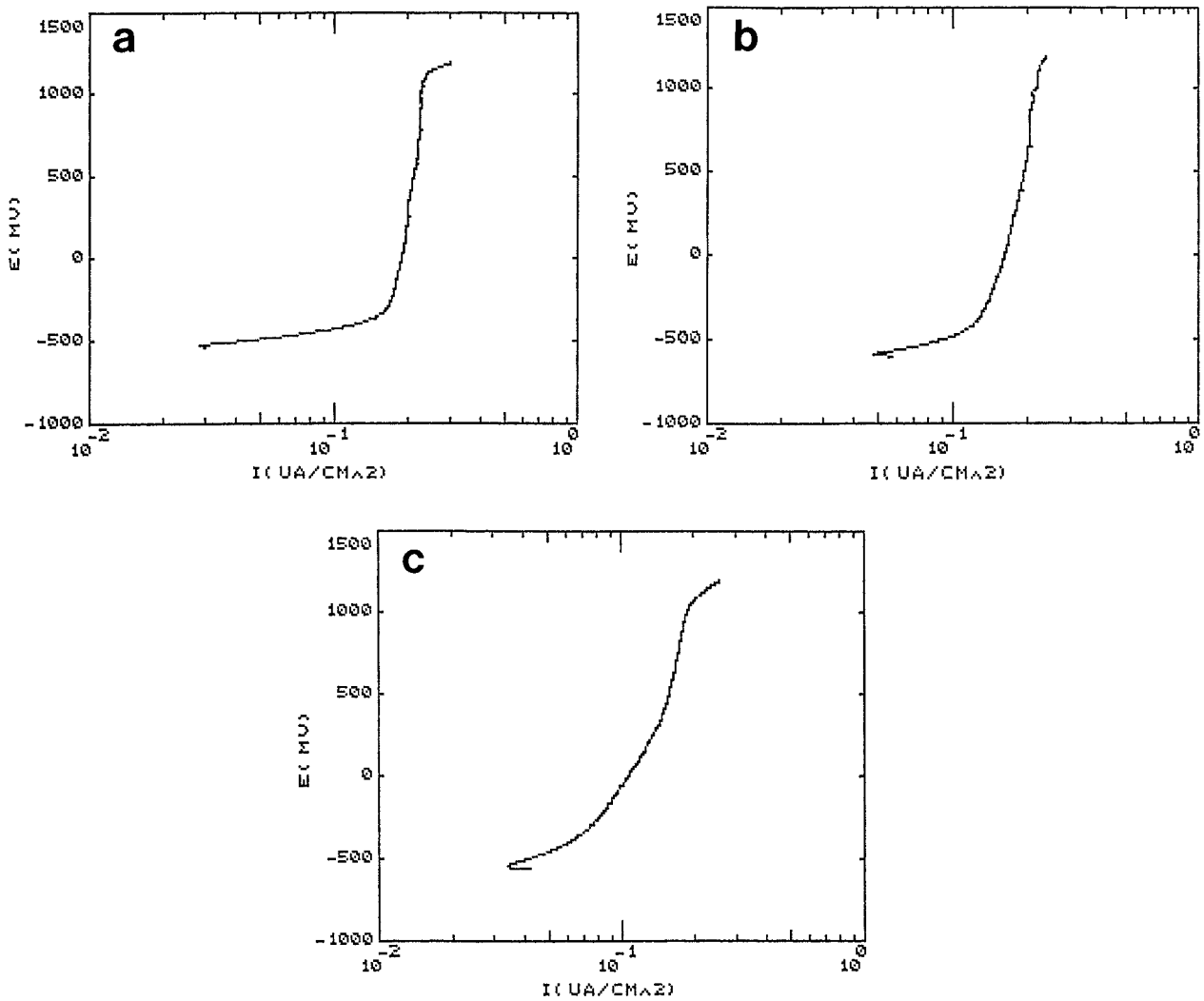

Figure 1 Potentiodynamic scans for the (a) Ti40Ta, (b) Ti50Ta and (c) Ti6A14V materials in the as-received condition. The TiTa alloys agree very well with the Ti6A14V material.

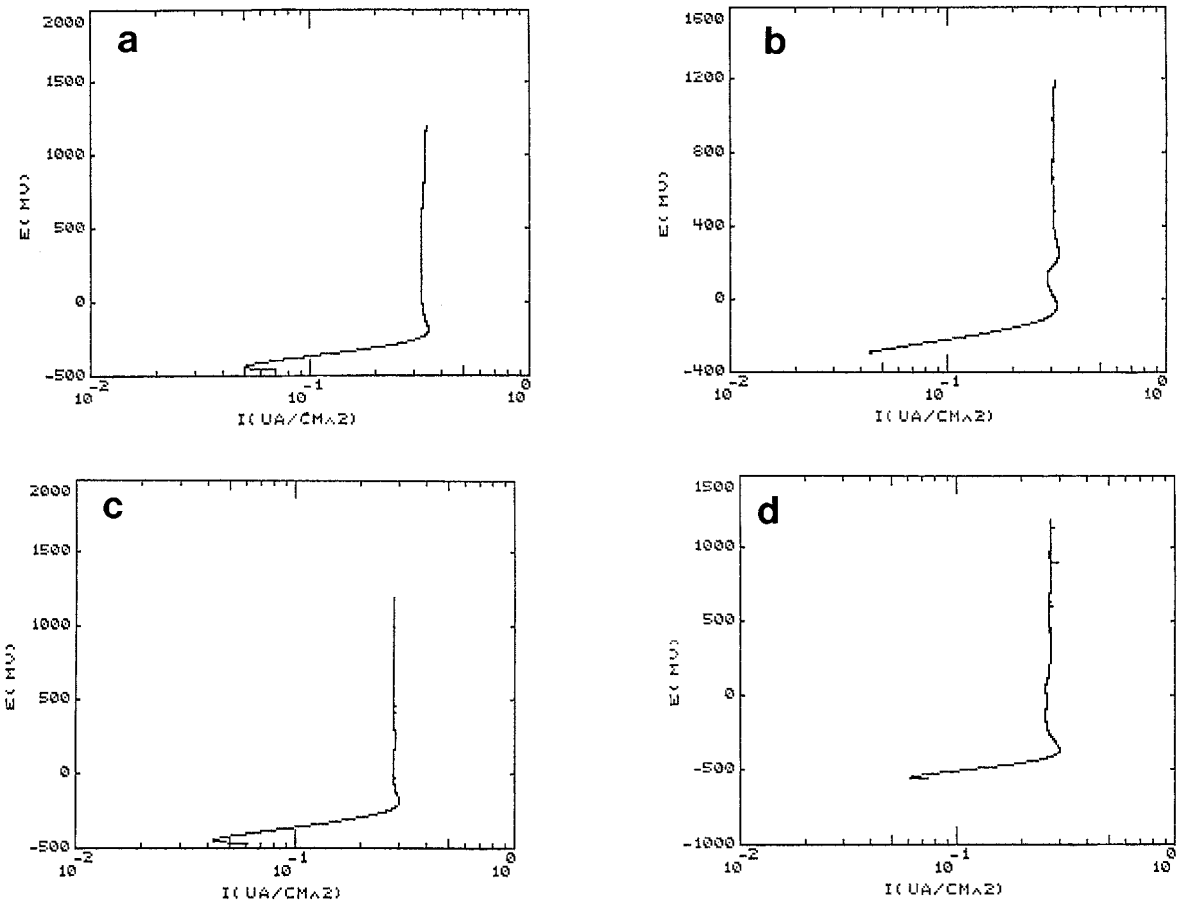

Figure 2 Potentiodynamic scans for the 1000 °C heat-treated samples. (a) Ti40Ta – quenched, (b) Ti50Ta – quenched, (c) Ti40Ta – furnace cooled, and (d) Ti50Ta – furnace cooled. All scans show very stable passive layers at low current densities.

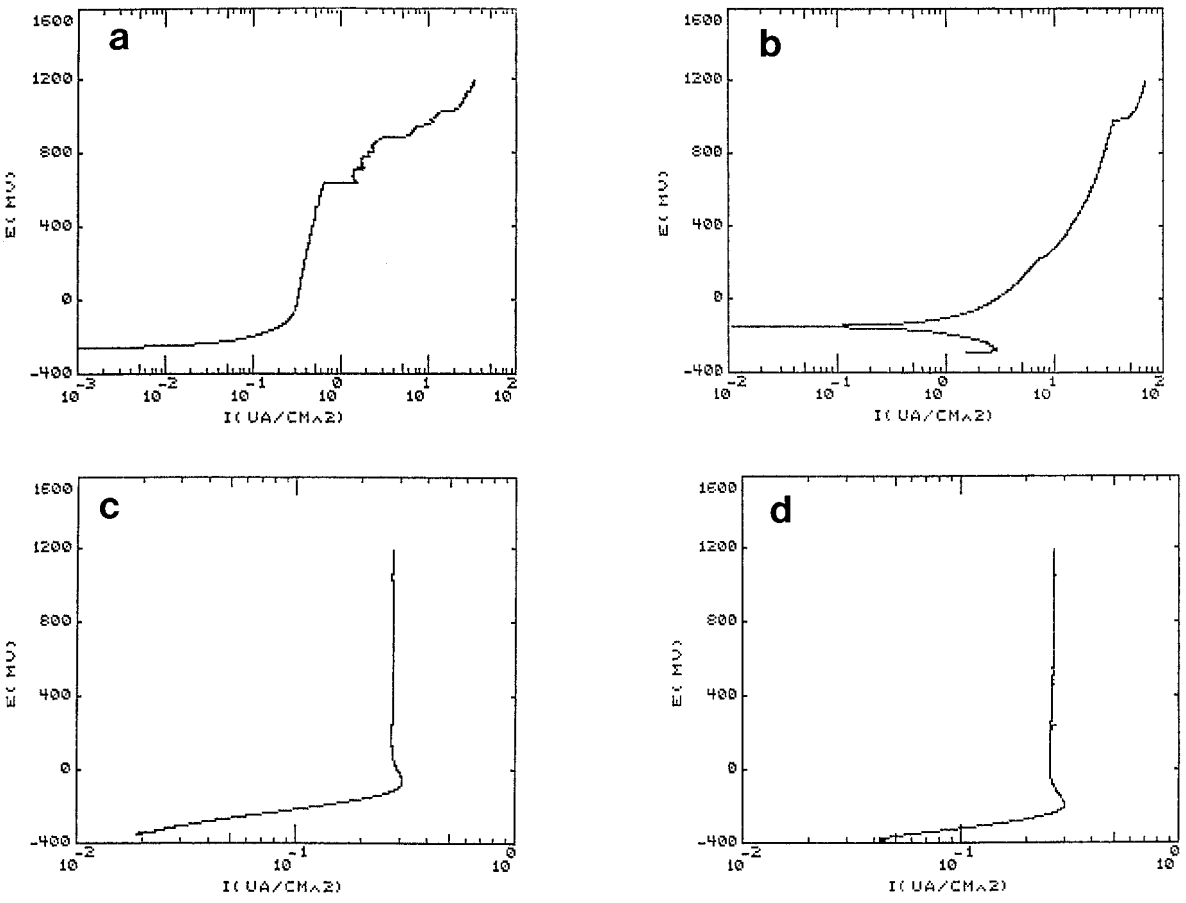

Figure 3 Potentiodynamic scans for the samples aged at 400 °C. (a) Ti40Ta – 3 h, (b) Ti50Ta – 3 h, (c) Ti40Ta – 10 h, and (d) Ti50Ta – 10 h.

treated samples (5×10^{-1} vs 1×10^{-1} μA/cm^2). In addition, the 3 h Ti40Ta sample shows a much lower pitting potential than all other samples (650 mV). Of all the samples analyzed the Ti50Ta treated for 3 h (Fig. 3b) is the least promising from a corrosion perspective. The passive layer breaks down and forms again repeatedly. The passive currents are two orders of magnitude higher than all other samples (1×10^{1} μA/cm^2). On the other hand, the Ti40Ta and Ti50Ta materials heat-treated for 10 h (Fig. 3c and d) both show extremely stable and steep passive slopes whose passive currents are comparable to the as-received and 1000 °C treated samples.

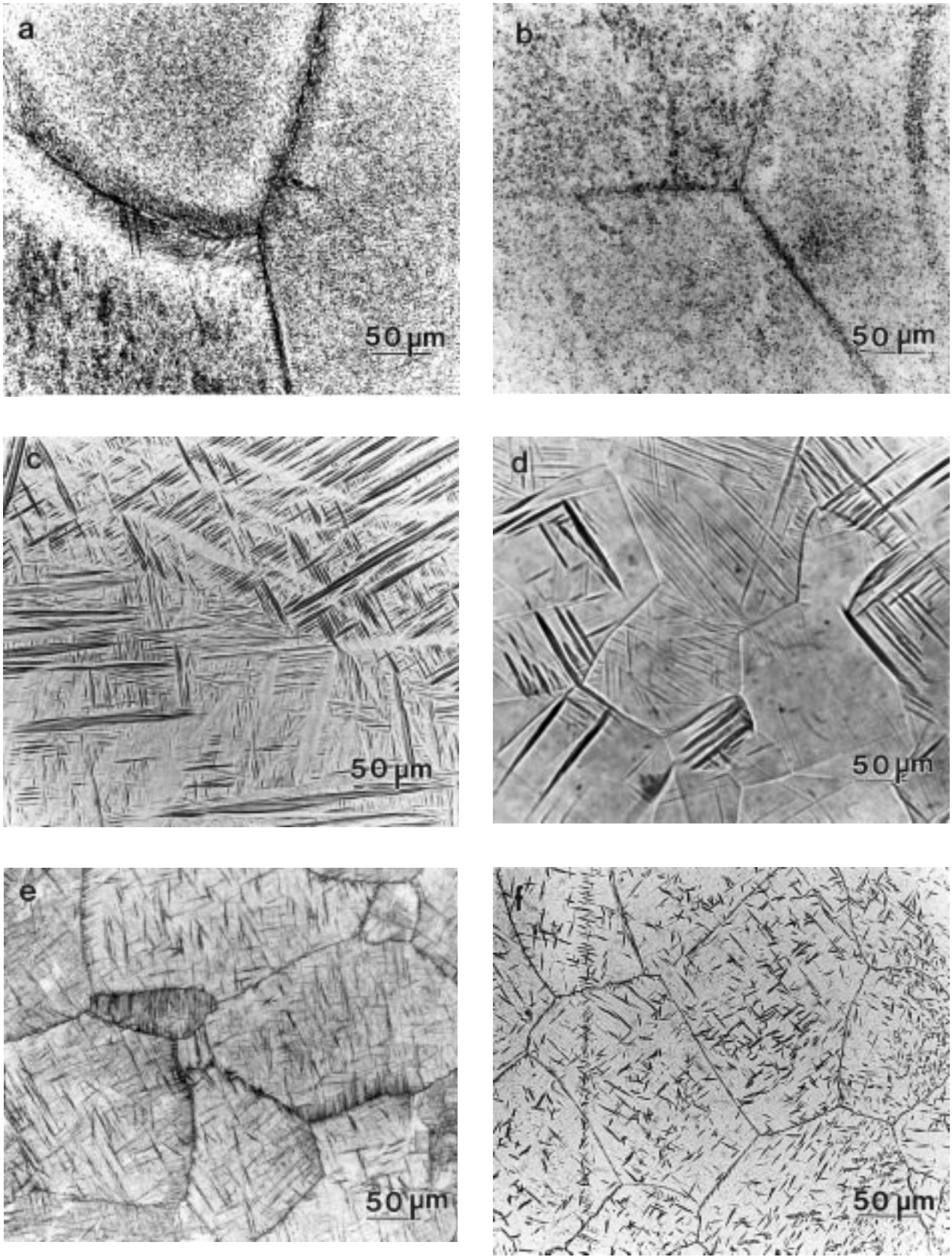

Figure 4 Optical micrographs for the as-received (AR) and 1000 °C treated samples. The (a) Ti40Ta and (b) Ti50Ta – AR materials show an α precipitate in an α + β matrix. The (c) Ti40Ta and (d) Ti50Ta quenched samples show large martensite laths whereas the (e) Ti40Ta and (f) Ti50Ta furnace cooled samples show smaller whisker-like martensite.

Optical micrographs of the surface structure are seen in Figs 4 and 5. Although the as-received and 1000 °C treated samples display similar polarization curves (Fig. 1) they demonstrate drastically different microstructures. Both as-received Ti40Ta and Ti50Ta (Fig. 4a and b) show an α precipitate phase in the α + β grain matrix, however, the Ti40Ta sample shows a higher density of α precipitate at the grain boundaries. It is also interesting to note that there is an α alignment at the grain boundaries in the Ti40Ta samples that is not observable in the as-received Ti50Ta samples. The 1000 °C quenched samples contain martensite laths that are more visible in the Ti40Ta sample (Fig. 4c). The samples that were heat-treated at 1000 °C and furnace cooled show needle-like martensite laths that seem to be more elongated in the Ti40Ta case (Fig. 4e). Also, some α is still observable in the α + β matrix in the Ti50Ta sample (Fig. 4f).

The samples aged at 400 °C for 3 and 10 h, respectively are shown in Fig. 5. The 3 h treated samples both show an α phase in the matrix and at the grain boundaries. The Ti50Ta sample, however, shows an observable increase in the density of aligned α at the grain boundaries than the Ti50Ta as-received sample (Figs 5b and 4b respectively). The Ti50Ta 10 h sample shows an even more extensive grain boundary alignment (Fig. 5c).

The TEM microstructure of the as-received Ti40Ta and Ti50Ta samples are seen in Fig. 6. The α phase is surrounded by an α + β phase in both instances (Fig. 6a and b). There is also a martensite phase visible that is more feather-like in appearance in the Ti40Ta samples (Fig. 6c), whereas the Ti50Ta material has a more band-like structure (Fig. 6d). The Ti6A14V as-received material in Fig. 6e reveals a very small single phase grain structure with a heavy dislocation density. The samples heat-treated at 1000 °C and then quenched show a pure martensite phase in both the Ti40Ta and Ti50Ta samples. The bands of martensite are intertwined and often change direction. Also, thick martensite bands are often interrupted by smaller bands (Fig. 7a and b). Both furnace cooled alloys display massive α precipitates that are surrounded by α + β and martensite phases (Fig. 7c and d).

The samples aged at 400 °C also show the α precipitates. However, the α is much more elongated than in the furnace cooled treatment. The Ti50Ta

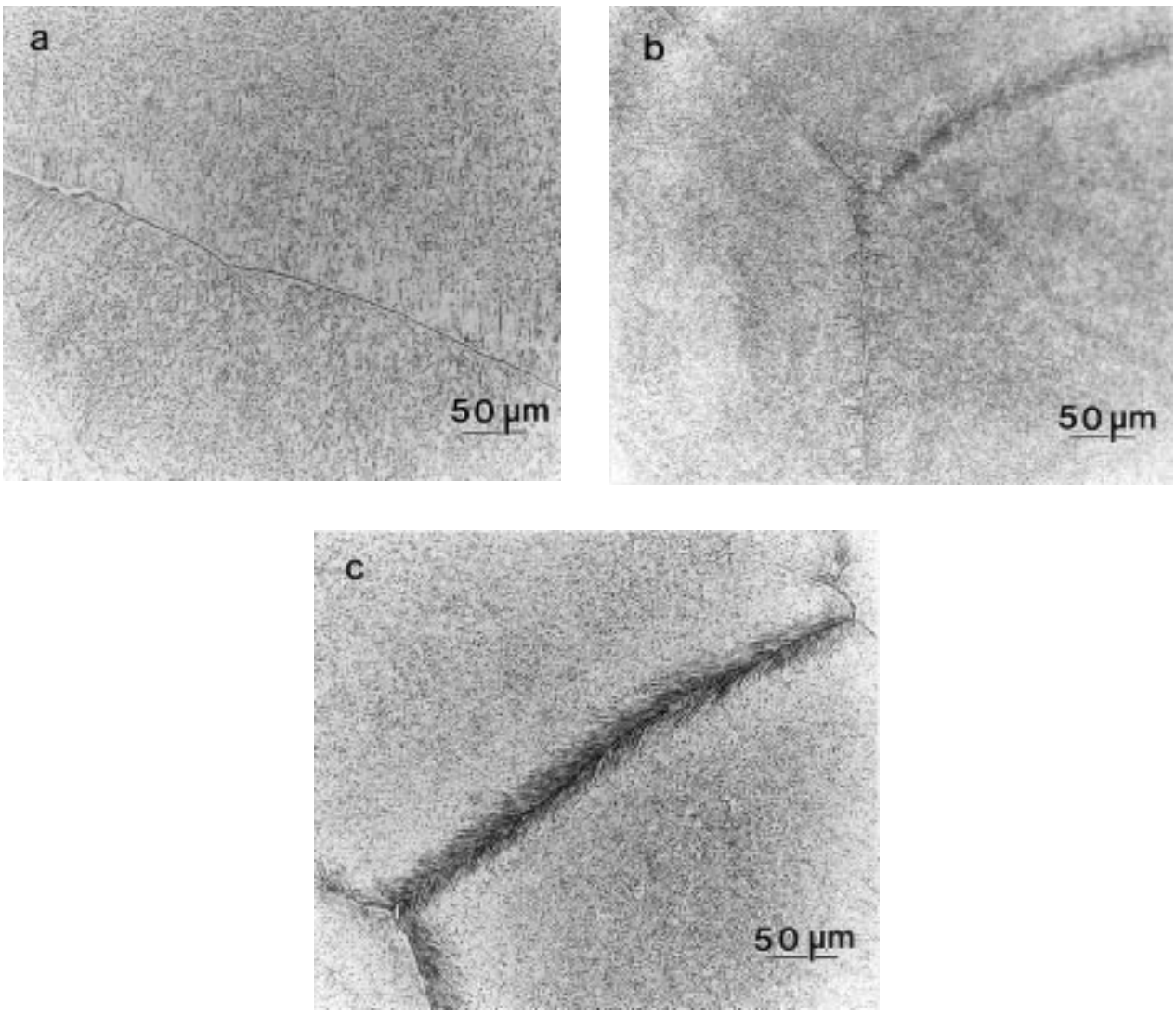

Figure 5 Optical micrographs for the samples aged at 400 °C. (a) Ti40Ta – 3 h, (b) Ti50Ta – 3 h, (c) Ti50Ta – 10 h. The α precipitates show an alignment at the grain boundaries.

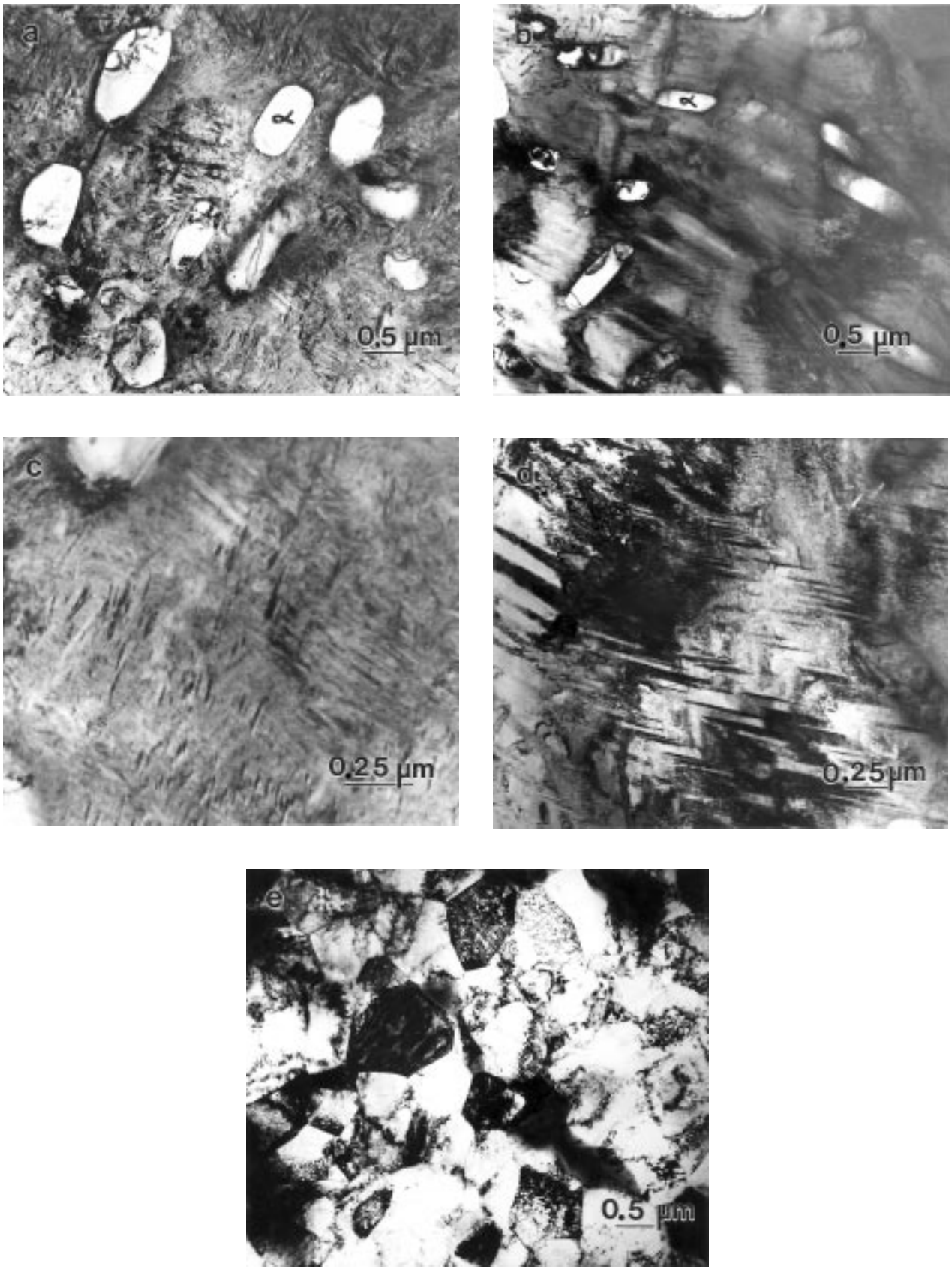

Figure 6 TEM micrographs of the as-received (a) and (c) Ti40Ta, (b) and (d) Ti50Ta, and (e) Ti6A14V materials. As-received TiTa alloys show α precipitates in an α + β and martensite matrix.

samples heat treated for 3 and 10 h (Fig. 8b and d) prominately show the ability of the precipitate to elongate after aging. Both the 3 h samples and the Ti50Ta 10 h sample have an α + β matrix surrounding the α precipitate. The Ti40Ta sample (Fig. 8c) heat-treated for 10 h display mostly one single parent phase, an aspect which will be discussed in the next section.

The results of the Vickers microhardness tests are recorded in Table II for both experimental materials, and for all heat-treatment conditions. The Ti6A14V material

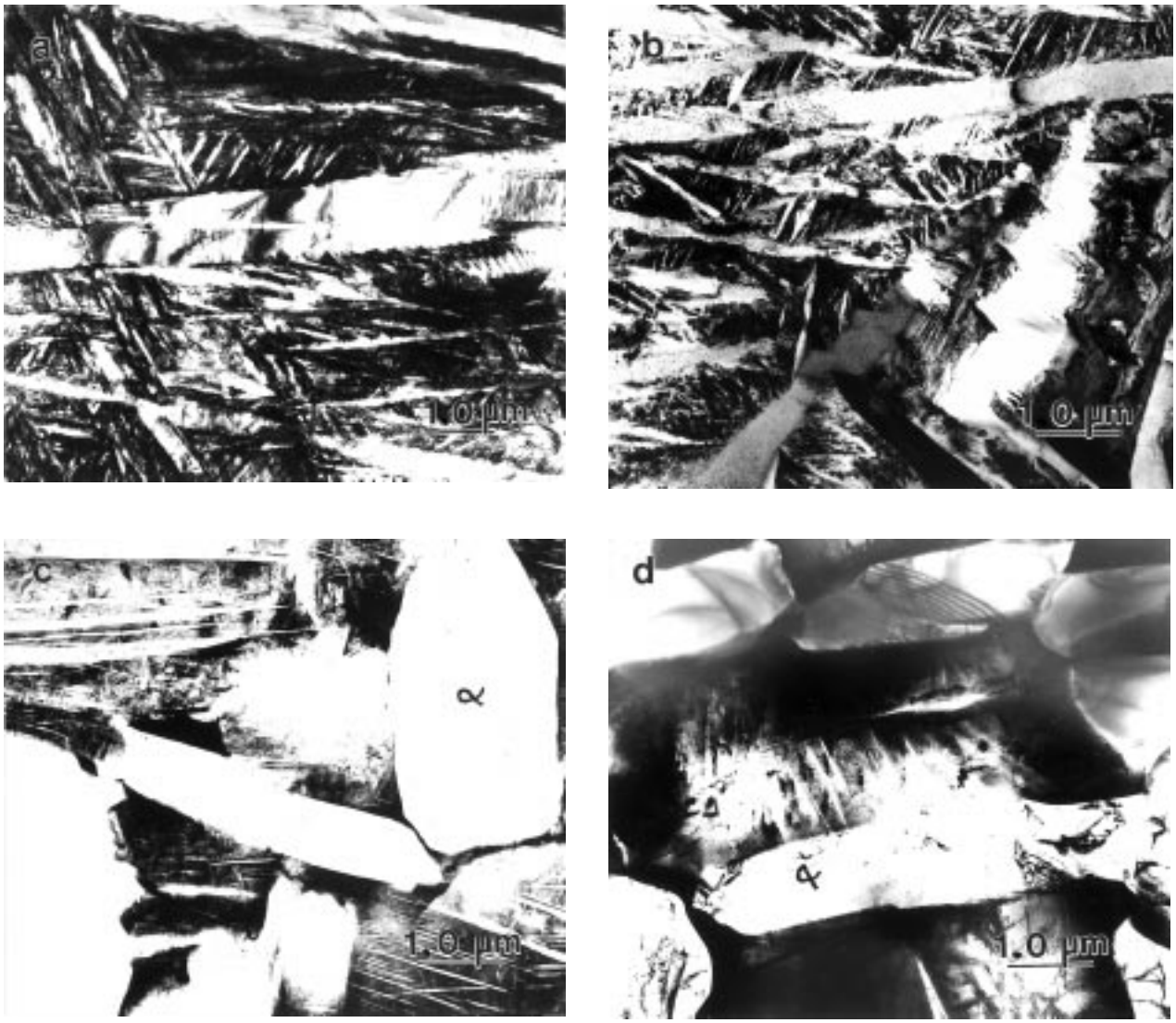

Figure 7 TEM micrographs of the 1000 °C heat-treated samples. (a) Ti50Ta – quenched, (b) Ti50Ta – quenched, (c) Ti40Ta – furnace cooled, and (d) Ti50Ta – furnace cooled. The quenched samples show a purely martensitic phase whereas the furnace cooled samples show a mixture of large α, α + β, and martensite.

was also included for comparison. It can be seen that all materials meet the requisite tensile strengths for implantation. The Ti50Ta sample heat treated at 400 °C for 10 h yields the highest hardness and tensile (strength) values. As shown in Fig. 1 this alloy and aging conditions also demonstrated superior corrosion inhibition.

4. Discussion

The two TiTa alloys (Ti40Ta and Ti50Ta) responded very well to the corrosion (potentiodynamic) tests performed in a simulated biological solution. All heat-treatment conditions except for the Ti50Ta aged at 400 °C for 3 h meet or surpassed the corrosion capability of Ti6A14V, which was used as a biomaterial standard. The differing microstructures of these alloys could not account for this anomaly. Several tests on the same material have only provided the same anodic behavior. It should be noted, however, that the surface roughened somewhat during polishing of these alloys, thus obtaining a perfectly smooth sample finish was very difficult. Surface analysis will be performed to determine if the surface roughening played a role in the differing polarization curve.

The estimated tensile strengths of these Ti–Ta alloys look quite promising for most of the heat-treatment conditions. The Ti40Ta and Ti50Ta as-received materials both display higher tensile strengths when compared to Ti6A14V (786, 724 and 689 MPa, respectively) which represent a 14% and 8.9% increase over the Ti6A14V material. Although the quenched samples did not produce an increase in the tensile strengths the furnace cooled samples did. The Ti40Ta increased nearly 7% in estimated strength in the furnace cooled state over the as-received state. The Ti50Ta furnace cooled material increased 21.8% from the as-received condition. They show an improvement of 22% and 28% in tensile values over the Ti6A14V material. It may be that the α phase is much harder than the martensite phase, which is what predominated at the furnace cooled state. The aging experiments have shown that the enhanced α phase produces higher tensile strengths for all cases when comparing it to the as-received and Ti6A14V materials. The Ti40Ta and Ti50Ta materials aged for 3 h increase 14.8% and 48.5% in tensile strength over their respective as-received counterparts, and 31% and 56% over the Ti6A14V sample. The Ti40Ta 10 h specimen only

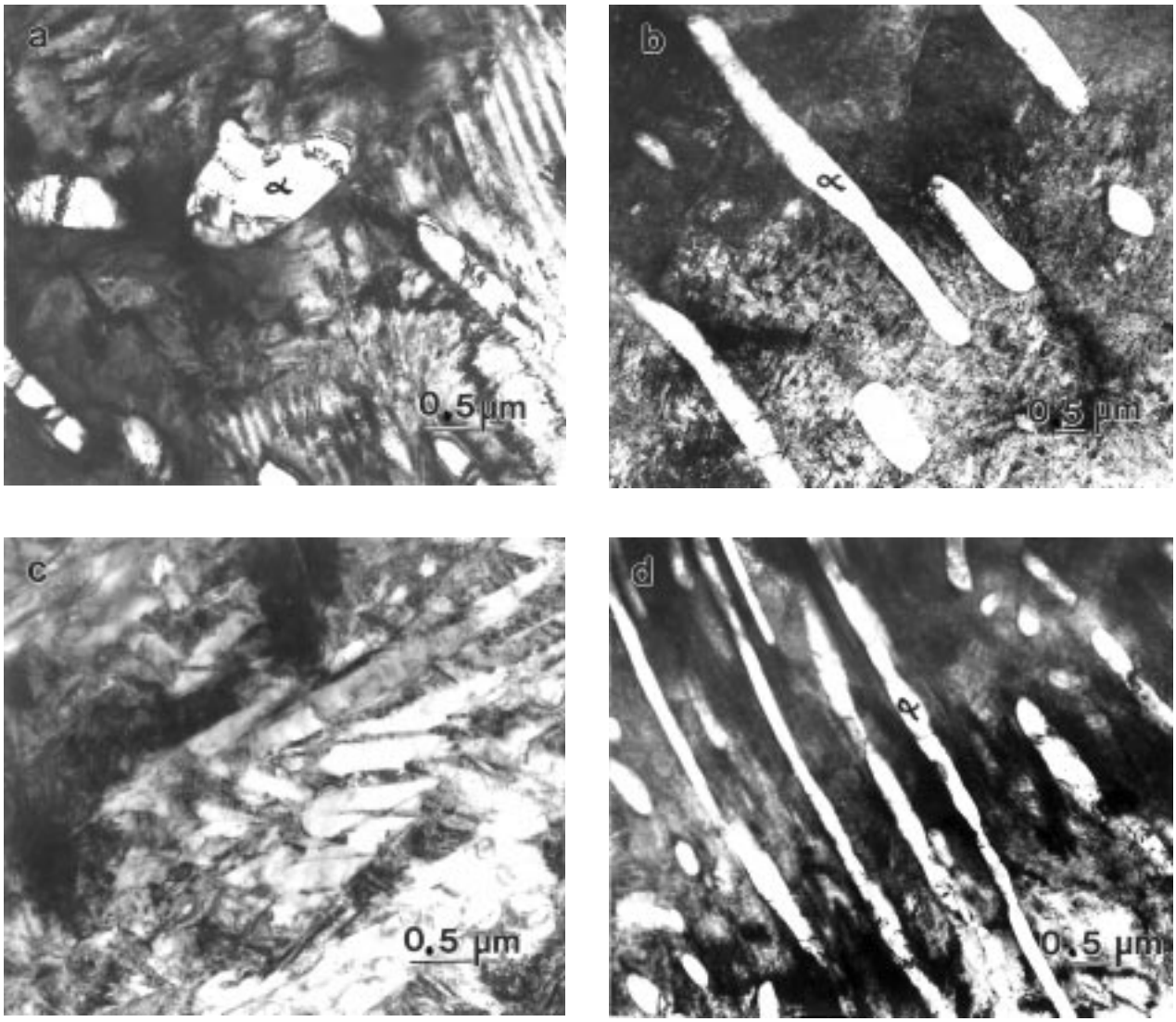

Figure 8 TEM micrographs of the 400 °C aged specimens. (a) Ti40Ta – 3 h, (b) Ti50Ta – 3 h, (c) Ti40Ta – 10 h, and (d) Ti50Ta – 10 h. Aging experiments have produced an elongated α microstructure except for the Ti40Ta – 10 h sample.

showed an increase of 3.4% over the as-received and an 18% increase over the Ti6A14V material. The Ti50Ta 10 h sample on the other hand had the highest increase over its as-received state and Ti6A14V materials (50.4% and 58%). The reason for a lower temperature aging experiment was due to the observed α phase precipitate alignment on the Ti40Ta as-received sample. It was our intention to increase the amount of α at the grain boundaries to see if this influenced corrosion behavior. This attempt was successful at least for the Ti40Ta 3 h treatment and the 10 h treatments as can be seen by the optical and TEM micrographs (Figs 4b, 5b and 5c). Comparing the Ti50Ta samples in the as-received state to the aging experiments seen in Fig. 9, we can see the progression of the elongation of the α phase. This elongated α microstructure causes an increase in the Vickers microhardness values: 320, 469 and 475 which corresponds to strength values of 724, 1075 and 1089

TABLE II Vickers microhardness values translated to tensile strength

Sample	Vickers	Brinell	TS, ksi/MPa
Ti6A14V – AR	306	287	100/689
Ti40Ta – AR	348	327	114/786
Ti50Ta – AR	320	300	105/724
Ti40Ta – Q	265	256	90/620
Ti50Ta – Q	278	265	93/641
Ti40Ta – FC	370	349	122/841
Ti50Ta – FC	386	365	128/882
Ti40Ta – 3 h	394	373	131/903
Ti50Ta – 3 h	469	446	156/1075
Ti40Ta – 10 h	358	337	118/813
Ti50Ta – 10 h	475	452	158/1089

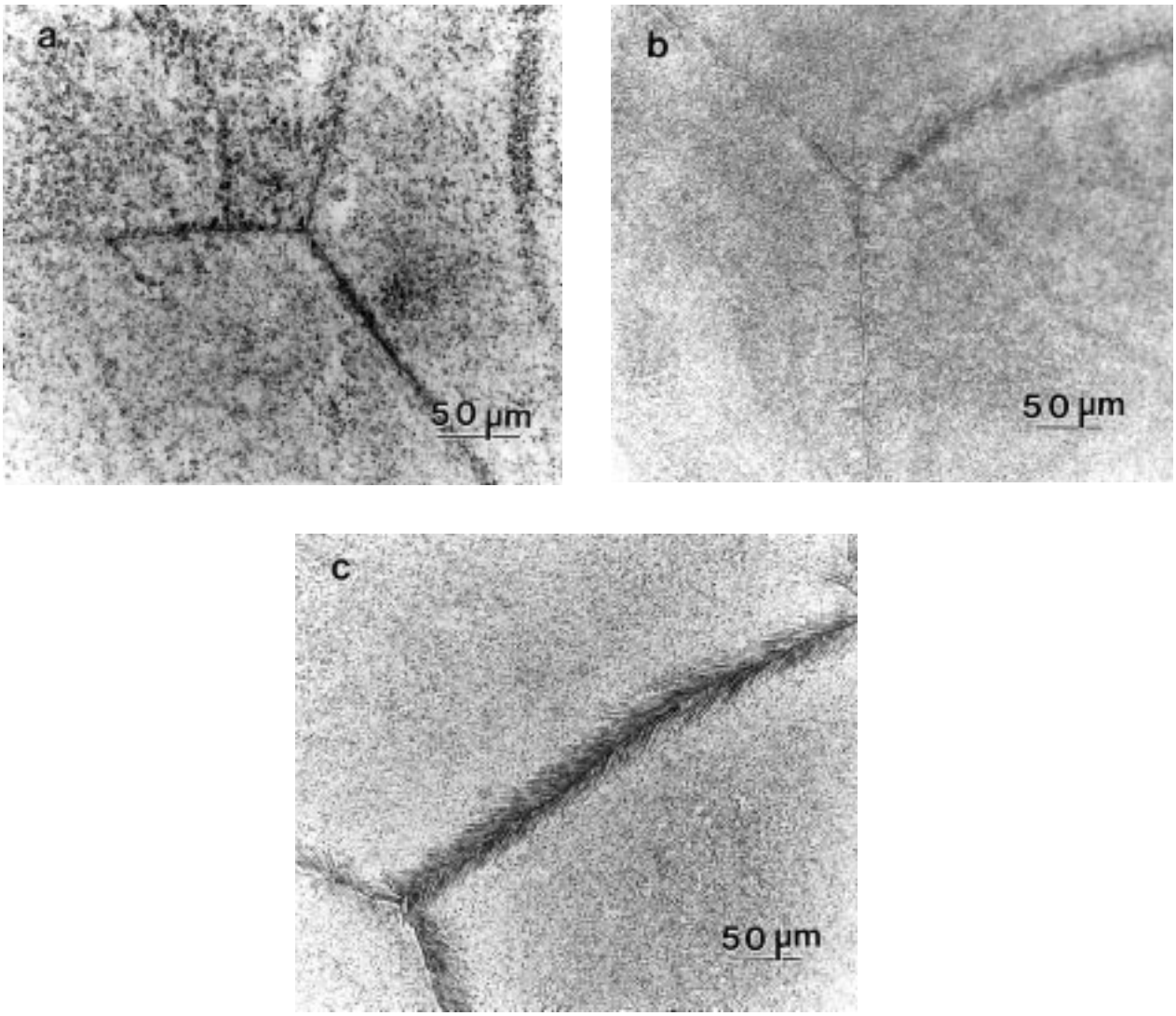

Figure 9 Optical micrographs of the Ti50Ta samples in the (a) as-received, (b) 3 h, and (c) 10 h heat-treatment conditions. Aging of this material has enhanced the α precipitate to a more elongated morphology.

MPa, respectively. The aging experiments produced a change in precipitate morphology to a more elongated α microstructure, which could certainly have affected the hardness. Thus this enhanced α microstructure not only improved the strength of the material but often resulted in better corrosion resistance. The Ti50Ta material aged at 10 h was the most promising of all materials that were examined because it gave the best tensile strength (1089 MPa) with excellent corrosion resistance. The Ti40Ta heat-treated at 400 °C for 10 h was the only aging experiment which did not produce an α-aligned microstructure as was observed through TEM microscopy. A single phase Ti microstructure was produced instead which was due to nonhomogenous fabrication for that one sample.

5. Conclusions

The following conclusions may be drawn from this research program:

1. Then potentiodynamic tests resulted in a stable passive layer at low current densities for all heat-treatment conditions except for the Ti50Ta specimen aged at 400 °C for 10 h. In addition, these samples were comparable to the corrosion capability of Ti6A14V, which was our biomaterial standard.

2. Ti40Ta and Ti50Ta as-received specimens contained a microstructure that consisted of α precipitates in an $\alpha + \beta$ matrix, along with bands of martensite. Quenched samples showed a pure martensitic phase whereas the furnace cooled samples show a massive α precipitate structure in an $\alpha + \beta$ and martensite matrix.

3. The Ti40Ta and Ti50Ta materials aged at 400 °C for 3 and 10 h produced a more elongated α-precipitate microstructure that increased in length with heat-treatment time, except for the Ti40Ta a 10 h sample.

4. The aged Ti40Ta and Ti50Ta samples provided the highest tensile strengths of all the samples tested, except for the 10 h Ti40Ta sample. This increase in strength was attributed to the enhanced α microstructure.

5. The Ti50Ta aged 10 h alloy is much more corrosion resistant and is 58% harder/stronger than Ti6A14V. The enhanced α precipitate microstructure produced by aging the sample apparently contributes significantly to the macroscopic properties of the material.

Acknowledgments

We gratefully acknowledge Bill M. Hogan at the Los Alamos National Laboratory for the TiTa materials. This research is funded through the Defense Logistics Agency (DLA) through the Defense National Stockpile Center Project-DN–009; and a General Services Administration (GSA) Grant PF-90-018.

References

1. P. D. BIANCO, P. DUCHEYNE and J. M. CUCKLER, *J. Mater. Sci: Mater. Med.* **8** (1997) 525.
2. A. B. FURGUSON, Jr. P. G. LAING and E. S. HODGE, *J. Bone Jt. Surg.* **42A** (1960) 76.
3. P. D. BIANCO, P. DUCHEYNE and J. M. CUCKLER, *J. Biomed. Mater. Res.* **31** (1996) 227.
4. P. DUCHEYNE, G. WILLEMS, M. MARTENS and J. HELSEN, *ibid.* **18** (1984) 293.
5. G. MEACHIM and D. F. WILLIAMS, *ibid.* **17** (1973) 555.
6. H. J. AGINS, N. W. ALCOOK, M. BANSAL, E. A. SALVANTI, P. D. WILSON, Jr, P. M. PELLICCI, and D. G. BULLOUGH, *J. Bone Jt. Surg.* **70A** (1988) 347.
7. L. D. DORR, R. BLOWBAUM, J. EMMANUAL and R. MELDRUM, *Clin. Orthop.* **261** (1990) 82.
8. J. KARRHOLM, W. FRECH, F. SNORRASON and K. G. NILSSON, *Trans. Orthop. Res. Soc.* **18** (1993) 507.
9. M. S VERANI, G. W. GUIDRY, J. J. MAHAMARIAN, S. NISHMURA, T. ATHANASOULIS, R. ROBERTS, and J. L. LACY, *J. Am Coll. Cardiol.* **20** (1992) 1490.
10. W. JASCHKE, K. J. KLOSE and E. P. STRECKER, *Cardiovasc. Intervent. Radiol.* **15** (1992) 356.
11. H. PRIGENT, P. PELLEN-MUSSI, G. CATHELINEAU and M. BONNAURE-LALLET, *J. Biomed, Mater Res.* **32** (1998) 200.

Received 10 June
and accepted 14 December 1999